FT-IR Study of Orientation Relaxation in Uniaxially Oriented Monodisperse Atactic Polystyrenes

André Lee and Richard P. Wool*

Polymer Group, Department of Metallurgy and Mining Engineering, University of Illinois, Urbana, Illinois 61801. *Received September 9, 1985*

ABSTRACT: Fourier transform infrared (FT-IR) dichroism was used to study the relaxation of molecular orientation in uniaxially step strained near-monodisperse molecular weight atactic polystyrene films at temperatures above the glass transition. The orientation relaxation process was analyzed in terms of the minor-chain reptation model for polymer melts. The model predicts that the normalized Hermans orientation function, F, depends on the relaxation time, t, and molecular weight, M, as $F = 1 - \alpha t^{1/2} M^{-3/2}$, for $t < T_r$, where α is a proportionality constant and T_r is the reptation time. Excellent agreement with experiment was obtained for molecular weights up to 4×10^5 above the critical entanglement molecular weight. Furthermore, the FT-IR method allows a direct measurement of T_r, and it was found that $T_r \sim M^3$ in agreement with the reptation prediction of de Gennes. Deviations from the predicted behavior are observed for $M \simeq 10^6$ and are discussed in terms of Rouse and reptation dynamics.

Introduction

Many applications of polymeric materials depend on how well one understands the response of polymers during mechanical deformation. The behavior of amorphous polymers in an entangled medium has interested polymer scientists for a long time. During the last 10 years much progress has been made due to the introduction of the "tube" concept.[1-3] The entangled polymer chain can rearrange its conformation by reptation, in which curvilinear diffusion of the chain along the chain contour occurs in the presence of entanglements and topological constraints. Two well-known predictions from the reptation model are

$$D \sim M^{-2} \tag{1}$$

and

$$T_r \sim M^3 \tag{2}$$

where D is the center-of-mass self-diffusion coefficient, T_r is the time for rearrangement of its conformation to about 70% of its initial value, and M is the molecular weight of the polymer.

In this paper, we propose the use of infrared dichroism to observe the orientation relaxation in uniaxially strained atactic polystyrene samples. We believe that the orientation of the strained polymer chain is relaxed by the emergence of the minor chain from its initial "tube". The minor chain loses the memory of its initial orientation and forms a randomly oriented Gaussian coil. The motion of the minor chain and the orientation relaxation process are discussed under Theory, as are the time and molecular weight dependence of the orientation function. In addition, the concepts of the infrared dichroism technique are also discussed. The "start-stop" experimental technique is used to improve the signal-to-noise ratio of infrared absorption. In the fourth section, the experimental results are presented in terms of the normalized Hermans orientation function and compared with the predictions of the minor-chain reptation model. Conclusions of this study are made in the last section.

Theory

Minor-Chain Reptation Considerations. In an amorphous polymer melt, the motion of a chain is greatly restricted due to its entanglement with neighboring chains. According to the reptation model,[1-3] the entanglements effectively confine the chain inside a tube-like region, while the chain can wriggle around inside the tube due to thermal fluctuations. de Gennes[1] argues that any wriggling motion is both rapid and small in magnitude; therefore, over a long time scale, the chain, on average, moves coherently back and forth along the center line of the tube with a certain diffusion constant, keeping its arclength constant. Overall then, the entire chain executes a one-dimensional random walk along the tube. The chain conformation at a given moment is the same as the shape of the tube that confines the chain at that moment. The orientation relaxation process of an oriented chain behaves in a similar manner. After a relaxation time t, a fraction of the chain, $F(t)$, is still trapped in the initial tube and remains oriented while a fraction, $1 - F(t)$, has moved out of the initial tube and has returned to an isotropic state, as stated by de Gennes and Léger.[4] To show how a chain disengages itself from the initial tube, the chain conformations at different times are shown in Figure 1. In Figure 1, the initial tube (defined at time $t = 0$) is shown as two dotted lines at various times. At $t = t_1$, some end portions of the chain have already "escaped" from the initial tube. This portion of the chain is referred to as the minor chain.[5] The random coil spherical envelopes enclosing the minor chain at different times are shown in circles. The minor-chain portion forms a randomly oriented Gaussian coil and has lost its initial orientation. As the minor-chain portion increases, the initial orientation gradually relaxes.

The fraction of the chain, $F(t)$, trapped in the initial tube after a relaxation time, t, is given by the minor-chain model[5] as

$$F(t) = 1 - \frac{2\langle l \rangle}{L} \tag{3}$$

where L is the contour length of the chain and $\langle l \rangle$ is the length of the minor chain shown in Figure 1. The factor of 2 accounts for the two relaxed minor chains. The relaxed length $\langle l \rangle$ is given by[5]

$$\langle l \rangle \simeq 2\left(\frac{D^* t}{\pi}\right)^{1/2} \tag{4}$$

where $D^* = L^2/\pi^2 T_r$ is the one-dimensional curvilinear diffusion coefficient[1] and T_r is a characteristic relaxation (reptation) time. The approximation in eq 4 and subsequent derivations involves the condition that $t < T_r$.

Substituting for $\langle l \rangle$ and D^* in eq 3 gives the fraction of chain remaining in the initial tube as

$$F(t) \simeq 1 - \frac{4}{\pi^{3/2}}\left(\frac{t}{T_r}\right)^{1/2} \tag{5}$$

0024-9297/86/2219-1063$01.50/0

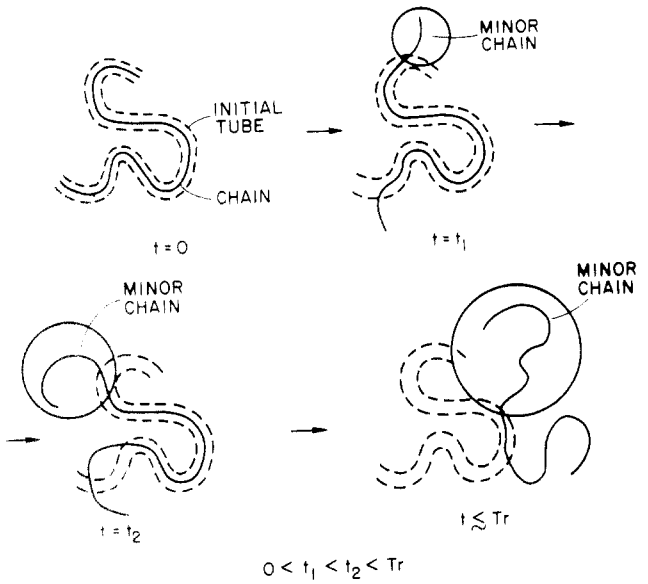

Figure 1. Disengagement of a chain from its initial tube and the emergence and growth of the minor-chain are shown. T_r is the tube renewal time.

Since $T_r \sim M^3$, the molecular weight dependence of $F(t)$ can be well approximated by[6]

$$F(t) \simeq 1 - \alpha t^{1/2} M^{-3/2} \tag{6}$$

where α is a temperature- and pressure-dependent proportionality constant. Thus, the minor-chain reptation model provides the exponents for both the time and molecular weight dependence of the relaxation process, which can be compared with experiment.

A complete expression for $F(t)$ has been obtained by several investigators[1,3,5,7-9] using a first-passage time analysis. Following de Gennes,[1] we have

$$F(t) = \frac{8}{\pi^2} \sum_{j=0}^{\infty} \frac{1}{(2j+1)^2} \exp\left(-(2j+1)^2 \frac{t}{T_r}\right) \tag{7}$$

It should be noted that T_r is proportional to, but not the same as, the complete tube escape time, T_s. They are related by[9] $T_s = (\pi^2/4)T_r$. Equation 7 has also been used by Doi and Edwards[3] to formulate a theory of linear viscoelasticity for polymer melts in which the stress relaxation modulus in shear is given by $G(t) = G_N^0 F(t)$, where G_N^0 is the terminal relaxation zone plateau modulus.

It can be shown[5,9] that eq 7 reduces to the more simple form for $F(t)$ given in eq 5 when $t < T_r$. Also, in eq 7 the first term ($j = 0$) of the infinite summation series provides the largest contribution to $F(t)$, particularly at long times ($t \geq T_r$), and a useful approximation is obtained as

$$F(t) \simeq \frac{8}{\pi^2} e^{-t/T_r} \tag{8}$$

Table I compares the approximate relations for $F(t)$ given by eq 5 and 8 with the exact relation, eq 7. When $t/T_r < 0.5$, eq 5 provides an excellent short-time description for $F(t)$ such that a plot of $F(t)$ vs. $t^{1/2}$ should be linear with a negative slope of $4/(\pi^{3/2}T_r^{1/2})$ and with an extrapolated intercept on the time axis at $t_0 = (\pi^3/16)T_r$. When $t/T_r > 0.5$, eq 8 provides a better long-time description for $F(t)$ such that a plot of log $F(t)$ vs. time should be linear with a negative slope of $1/T_r$. When T_r is known, eq 7 can then be used to provide an exact comparison of theory with experiment.

In the next section, we will explain the use of the infrared dichroism technique to examine the above relations for the orientation relaxation mechanism.

Table I
Comparison of Long-Times and Short-Times Approximations with the Exact Relation for the Fraction of Chain Remaining Inside the Initial Tube, $F(t)$

t/T_r	$F(t)$[a]	long-times approximation[b]	short-times approximation[c]
0	0.9996	0.8106	1
0.001	0.9773	0.8098	0.9773
0.002	0.9679	0.8089	0.9679
0.005	0.9492	0.8065	0.9492
0.007	0.9399	0.8049	0.9399
0.01	0.9282	0.8025	0.9282
0.02	0.8984	0.7945	0.8984
0.05	0.8394	0.7710	0.8394
0.07	0.8099	0.7558	0.8099
0.1	0.7728	0.7334	0.7728
0.2	0.6787	0.6636	0.6787
0.5	0.4926	0.4916	0.4920
0.7	0.4027	0.4025	0.3990
1.0	0.2982	0.2982	0.2817
1.5	0.1809	0.1809	0.1202
2.0	0.1097	0.1097	

[a] $F(t) = 8/\pi^2 \sum_{j=0}^{500} (1/(2j+1)^2) \exp(-(2j+1)^2 t/T_r)$. [b] $8/\pi^2 \times \exp(-t/T_r)$. [c] $1 - (4/\pi)(t/\pi T_r)^{1/2}$.

Infrared Dichroism Considerations. Vibrational spectroscopy, such as infrared or Raman spectroscopy, is a very useful tool for studying molecular motion as well as the orientation of polymers. The infrared absorption spectrum is obtained on the basis of the fact that the chemical group can only absorb the radiation of the same frequency as its natural vibrational frequency. Thus, we may examine many vibrational modes within the polymer at the same time. Infrared dichroism, or polarized infrared spectroscopy, is an established method of determining the degree of orientation in uniaxially oriented polymer systems. If the electric vector of incident radiation, **E**, is parallel to the transition dipole moment vector, μ, of a specific motion of vibration, the absorption intensity, A, of this vibration frequency is then at its maximum. However, if the electric vector is perpendicular to the transition dipole moment vector, the absorbance is 0. So, a nonvanishing scalar product of the transition dipole moment vector, μ, and the electric vector of the incident beam, **E**, is a necessary condition for polarized infrared absorption

$$A \sim (\mu \cdot \mathbf{E})^2 = K \cos^2 \alpha \neq 0 \tag{9}$$

where A is the absorbance, α is the angle between μ and **E**, and K is a constant independent of orientation. In a polymer system, the orientation of the individual chain segments and dipole-moment vectors can be distributed in some manner over all possible orientations. Therefore, the measured absorbance is an indication of an average overall orientation of the dipole-moment vectors for that particular vibration.

$$A \sim \langle (\mu \cdot \mathbf{E})^2 \rangle = K \langle \cos^2 \alpha \rangle \tag{10}$$

For any absorption band, the dichroic ratio $R = A_\parallel / A_\perp$ ($A_\parallel$ and $A_\perp$ being the measured absorbance for electric vector parallel and perpendicular, respectively, to the stretching direction) is related to the second moment of the orientation function $\langle P_2(\cos\theta) \rangle$ by[11]

$$f = \langle P_2(\cos\theta) \rangle = (3\langle \cos^2\theta \rangle - 1)/2 \tag{11}$$

and

$$f = \frac{R-1}{R+2} \frac{R_0+2}{R_0-1} \tag{12}$$

Table II
Near-Monodisperse Atactic Polystyrene from Pressure Chemical

weight-average mol wt, $\bar{M}_w$	degree of polydispersity, $\bar{M}_w/\bar{M}_n$	weight-average mol wt, $\bar{M}_w$	degree of polydispersity, $\bar{M}_w/\bar{M}_n$
170 000	1.04	390 000	1.06
233 000	1.04	600 000	1.14
300 000	1.04	900 000	1.08

with $R_0 = 2\cot^2\alpha$, where α is the angle between the dipole-moment vector of vibration and the chain axis, θ is the angle between the chain axis and the stretched direction, and f is called the Hermans orientation function.[12] This function has value of unity for complete alignment of the chain in the oriented direction and zero for a perfectly random orientation of the chain segments. Experimentally the angle α is usually difficult to obtain. Thus we have introduced a normalized form of this Hermans orientation function, F,

$$F = \frac{f_t}{f_i} = \frac{R_t - 1}{R_t + 2}\frac{R_i + 2}{R_i - 1} \tag{13}$$

where f_i and f_t are the Hermans orientation functions of the initial deformed state and at any time t later, respectively.

As described, in an entangled polymer melt, the emergence of the minor chain occurs by self-diffusion along the chain contour, and the minor chain forms a randomly oriented Gaussian coil as it loses the memory of its initial orientation. The normalized Hermans orientation function has value of unity at $t = 0$ and zero for complete relaxation. So, it is utilized here as a measure of the fraction of initial orientation that remains at time t.

Experimental Section

Sample Preparation. The near-monodisperse atactic polystyrene samples ($T_g \simeq 105$ °C) were supplied by Pressure Chemical. The weight-average molecular weight, $\bar{M}_w$, and degree of polydispersity, ($\bar{M}_w/\bar{M}_n$), are listed in Table II. PS films (5 mil thick) were prepared by dissolving in toluene and casting on a mercury surface. After the films were air-dried, the solvent was removed completely by heating the films at 100 °C in a vacuum for a day. The PS film was then cut into strips of length L_0 = 2.5 in. and width W_0 = 0.5 in. In order to provide a local macroscopic measurement of the draw ratio, small successive equidistant ink marks were engraved on the edge of the sample perpendicular to the stretching direction.

The uniaxial stretching was performed by using a servohydraulic tensile testing machine (MTS Model 820) equipped with a thermostatically controlled chamber set at a temperature of 115 ± 1 °C and gauge length of 1.5 in. The samples were first allowed to equilibrate to the oven temperature and then stretched in pure extension at a constant strain rate of 0.1 s^{-1} to an overall draw ratio, λ, (final gauge length/initial gauge length) of about 3.5. The specimen was then quickly quenched to room temperature, $T \ll T_g$, effectively freezing the orientation of the uniaxially deformed polymer chains. The draw ratio was uniform over a large region (~3 in.) in the middle of the extended sample at a value of $\lambda \approx 4$. The final width and thickness of the samples used in the experiments were proportional to the square root of the draw ratio, which is in good agreement with the assumptions of uniaxial stretching under constant volume conditions.

Orientation Relaxation Processes. Rapid orientation relaxation of an amorphous polymer can occur only at temperatures above its glass-transition temperature. Thus, the uniaxially deformed PS films were held at a fixed strain on a sample holder and then placed in an oven at a constant temperature of 114.6 ± 0.5 °C. At the end of each relaxation interval, the sample was quickly quenched to room temperature, effectively freezing the residual orientation of the polymer. We call this the "start-stop" method. The FT-IR polarized spectra were obtained in between each relaxation interval at room temperature.

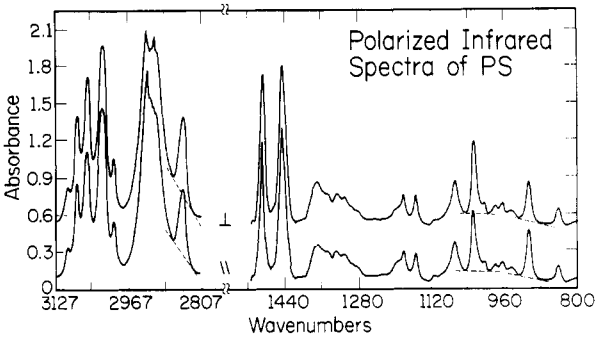

Figure 2. Survey-polarized infrared spectra of atactic polystyrene is shown.

Infrared Measurement. The infrared spectra were collected with a Nicolet 170 SX FT-IR spectrometer at 4-cm^{-1} resolution (NDP = 4096 data points, NTP = 8192 transform points). The parallel and perpendicular polarized spectra were obtained with a Perkin-Elmer gold wire grid polarizer. The measurement time for each polarized spectrum was about 4 min (NSS = 250 scans). The measurement time and the number of scans were determined such that the reproducibility was 0.2% or better for the dichroic ratio $R = A_\parallel/A_\perp$ of each vibrational frequency used in this study. The total absorption intensity of parallel ($A_\parallel$) and perpendicular ($A_\perp$) polarization was measured with respect to the orientation direction, and the total absorbance $A_0 = (A_\parallel + 2A_\perp)/3$ remained constant throughout the experiment. The normalized Hermans orientation function was then obtained through eq 13 by using the dichroic ratio measured at the end of each relaxation interval.

Results

In using the normalized Hermans orientation function, it is not required to make any assumptions about the angle between the dipole-moment vector and the chain axis. But, due to the different chemical groups' vibrational motion and the selection rules of polarized infrared absorption, some infrared absorption bands are more sensitive to the uniaxial stretching. Such vibrational modes give better reproducible, experimentally measurable dichroic ratios (Figure 2). Three well-analyzed vibrational modes of atactic polystyrene were chosen:[13] 906 cm^{-1} (out-of-plane mode $\nu_{17b}(B_1)$ of the aromatic ring), 1028 cm^{-1} (the ν_{18a} in-plane CH bending mode of the aromatic ring), and 2850 cm^{-1} (CH_2 symmetrical stretching vibration).

To compare the experimentally measured normalized Hermans orientation function with the minor-chain reptation model, we used eq 8 and plotted the log of the normalized Hermans orientation function vs. the relaxation time, as shown in Figures 3–5. For $\bar{M}_w \leq 390\,000$, we have excellent straight lines (the correlation coefficient $r^2 = 0.98$ or better) in the exponential curve fit. This is justified as we have listed in Table I, since the leading term of $F(t)$ contributed more than 95% to the infinite series value at $t/T_r \geq 0.1$. Thus, the slope of the exponential curve fit gives the inverse of the characteristic time, T_r, of orientation relaxation listed in Table III. In a self-consistent manner, we then plotted the normalized Hermans orientation function vs. t/T_r in Figure 6. Within experimental error, the normalized Hermans orientation functions for various molecular weights fall on a master curve, as described by eq 7.

The reptation model predicted the scaling arguments[1,10] that $T_r \sim M^3$. To test this relation we used the value of T_r listed in Table III and plotted it vs. the weight-average molecular weight, $\bar{M}_w$. This is shown in Figure 7. In this log T_r vs. log $\bar{M}_w$ plot, we used the least-square power curve fit and obtained a slope of 2.9, which is in good agreement with the prediction. But, because of the range of molecular weights (170 000–400 000), this is not necessarily sufficient

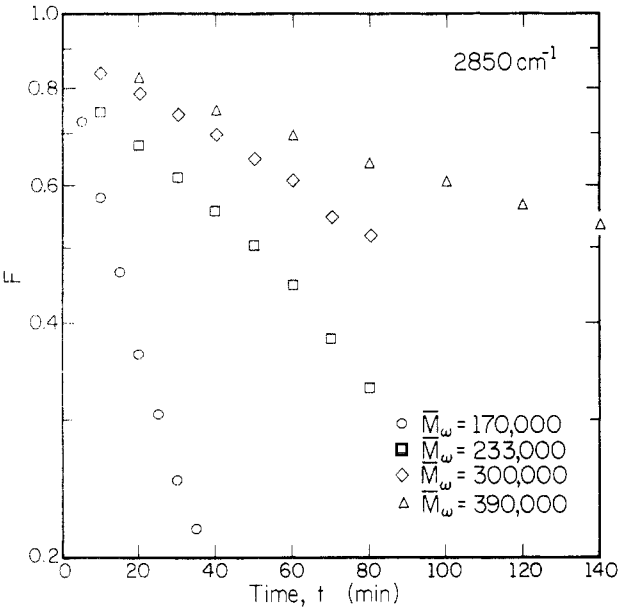

Figure 3. Normalized Hermans orientation function F vs. the relaxation time t is shown in a semilogarithmic plot. The 2850-cm^{-1} band is examined for various molecular weights at a constant strain and temperature of 114.6 °C.

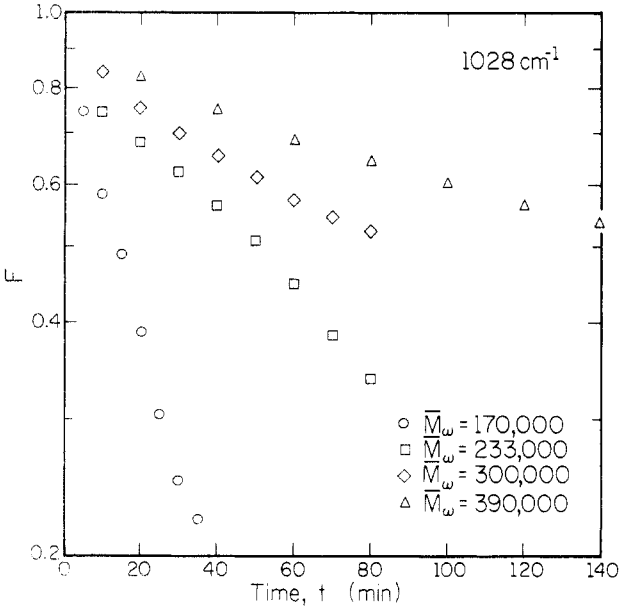

Figure 4. Normalized Hermans orientation function F vs. the relaxation time t is shown. The 1028-cm^{-1} band is examined for various molecular weights at a constant strain and temperature.

Table III
Characteristic Relaxation Time T_r and Escape Time T_s

$\bar{M}_w \times 10^{-3}$	ν, cm^{-1}	T_r, min	T_s, min $\equiv (\pi^2/4)T_r$
170	2850	24.5	60.5
170	1028	23.9	59.0
170	906	25.2	62.2
233	2850	87.3	215.4
233	1028	87.7	216.4
233	906	85.3	210.5
300	2850	146.2	360.7
300	1028	151.1	373.1
300	906	133.7	329.9
390	2850	287.9	710.4
390	1028	286.4	706.7
390	906	285.1	703.5

proof for the applicability of the reptation model to polymer melts.

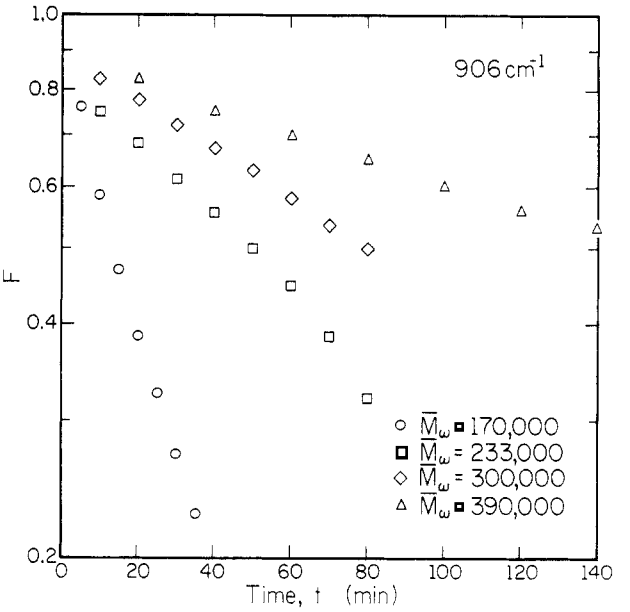

Figure 5. Normalized Hermans orientation function F vs. the relaxation time t is shown. The 906-cm^{-1} band is examined for various molecular weights at a constant strain and temperature.

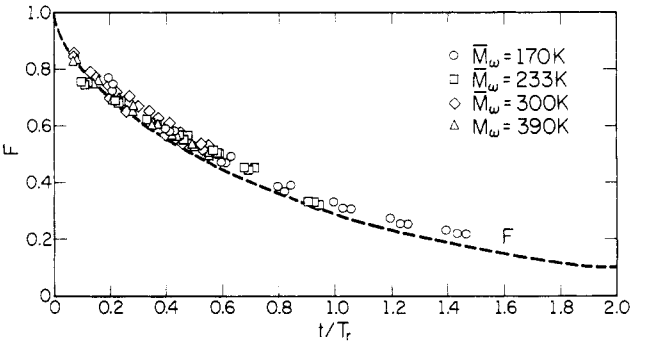

Figure 6. Normalized Hermans orientation function F vs. the normalized time t/T_r is shown. T_r is the characteristic relaxation time from Table III. It is compared with the master curve from the F of eq 7.

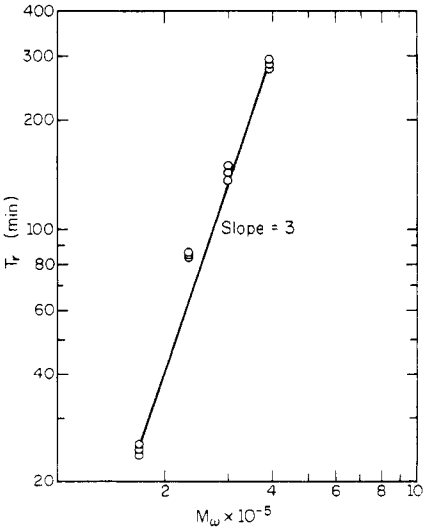

Figure 7. Log of the characteristic time T_r vs. the log of the weight-average molecular weight $\bar{M}_w$ is shown. A line with slope of 3 is shown.

To examine the scaling relations of the normalized Hermans orientation function, $F = 1 - \alpha t^{1/2} M^{-3/2}$ as shown in eq 6, we plotted ln $(1 - F)$ vs. ln (time) + ln $(\bar{M}_w)$. In Figure 8, the 1028-cm^{-1} band is plotted in this manner. For

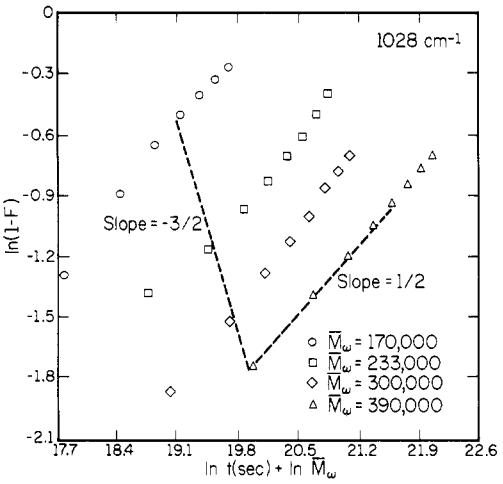

Figure 8. Ln $(1 - F)$ vs. ln (t) + ln $(\bar{M}_w)$ of the 1028-cm^{-1} band is shown. At $t \leq T_r$, good agreement with the scaling prediction $(1 - F) \sim t^{1/2}$ and $(1 - F) \sim M^{-3/2}$ (at 20 min) was observed.

the samples with $\bar{M}_w$ = 390 000 and 300 000, the experimental time is less than the characteristic time, T_r, and we observe a good agreement with the $t^{1/2}$ and $M^{-3/2}$ dependence, as in eq 5 and 6.

To further illustrate the complexities of the orientation relaxation process, we plotted the log of the normalized Hermans orientation function vs. the relaxation time for $\bar{M}_w$ = 600 000 and 900 000 (at T = 114.6 and 122.2 °C). Using the 2850-cm^{-1} band for illustration purposes (Figure 9), we noticed an initial rapid orientation relaxation, and then the orientation levels off to a plateau. The orientation functions of the plateau were different for different temperatures and molecular weights, but the slope of the initial orientation relaxation for both molecular weights was about the same.

Discussion and Conclusions

In this paper, we have presented experimental observations of orientation relaxation using FT-IR spectroscopy through the use of normalized Hermans orientation functions for near-monodisperse molecular weight amorphous polystyrenes. For $\bar{M}_w \leq$ 390 000, we have interpreted the experimental observations in terms of the minor-chain reptation model, and the experimental results supported these theoretical arguments. We observed that the normalized Hermans orientation function, F, at $t \ll T_r$ gives a $t^{1/2}$ and $M^{-3/2}$ dependence. In addition, the characteristic time T_r behaves as $T_r \sim M^3$, which further supports the scaling arguments.[10] The quantitative value of the complete disengagement time, T_s, is also in good agreement with Boue's small-angle neutron scattering experiments[15] and Tobolsky's stress relaxation experiments.[16]

However, for $\bar{M}_w >$ 400 000, the experimental data show some complexities and discrepancies with the minor-chain reptation model. Although it is difficult to pinpoint any reasons at this time, several possibilities may be considered:

(1) Effect of segmental orientation. In the present analysis, the orientation relaxation process of a strained polymer is assumed to be described by self-diffusion along the chain contour and the wriggling motion is completely neglected. However, the quantitative value of the Rouse time associated with the wriggling motion can be obtained from the published literature.[17,18] For $\bar{M}_w$ = 600 000 at T = 117 °C, the Rouse time is about 37 min, and for $\bar{M}_w$ = 900 000 at T = 117 °C, the Rouse time is about 83 min. This is close to the time that we observed near the slope

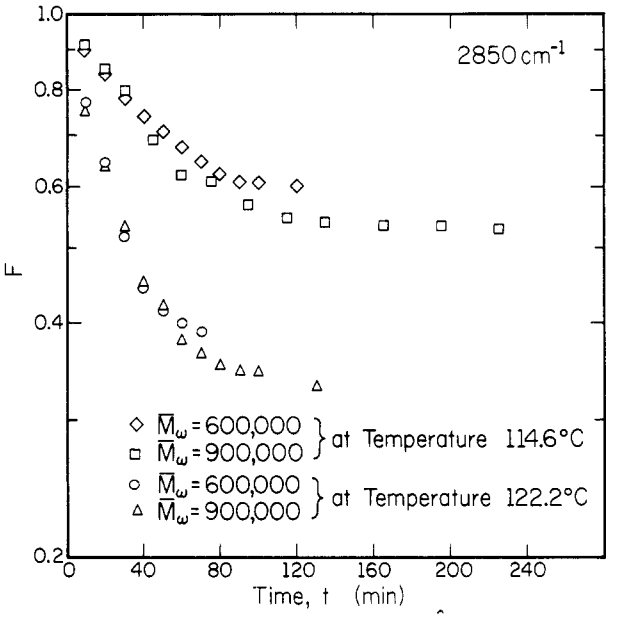

Figure 9. Normalized Hermans orientation function F vs. the relaxation time t is shown. The 2850-cm^{-1} bands of $\bar{M}_w$ = 600 000 and 900 000 atactic polystyrenes are used with a constant strain and two different temperatures.

transitions, as shown in Figure 9.

In terms of the reptation model, de Gennes[1] determined a time for equilibration of defects, $T_d \ll T_r$, which behaves as $T_d \sim M^2$, analogous to the Rouse relaxation time. Rouse-like segmental motion of the chain in its tube leads to the generation and propagation of "stored length defects" along the contour of the tube. If at $t = T_d$ the defects have equilibrated by the Rouse relaxation mechanism, further relaxation can then occur by the reptation mechanism at $t > T_d$. Thus, T_d represents a transition from the Rouse to the reptation relaxation mechanism. When we interpret our data in Figure 9 in the terms of this model and let T_d for the highest molecular weight sample at 114.6 °C be T_d $(9 \times 10^5) \approx 100$ min, then if $T_d \sim M^2$, the other samples have the following transition times: T_d $(6 \times 10^5) \approx 44$ min; T_d $(3.9 \times 10^5) \approx 18$ min; T_d $(3 \times 10^5) \approx 11$ min; T_d $(2.33 \times 10^5) \approx 7$ min; and T_d $(17 \times 10^4) \approx 4$ min. Note that in Figures 3–5 the majority of the data was evaluated in the reptation region at $t > T_d$ for each molecular weight. Comparing orientation relaxation data for the 2850-cm^{-1} band in Figures 3 and 9, it is clear that the same amount of relaxation did not occur during the interval $t < T_d$. Also in Figure 9 we note that at higher temperatures the extent of relaxation increases in the short-time region. This may be due to the ability of the molecules orientation to become more random locally with increasing temperature. It is conceivable that the molecule as a whole could lose most of its dichroism by local rearrangements before relaxing from its tube. The data in Figure 9 would seem to suggest that at even higher melt temperatures the infrared dichroism could be completely relaxed by segmental motion in a manner which would also be independent of molecular weight.

(2) Chemical irregularity of the samples. We have assumed that the polymer is a linear chain with δ-function molecular weight distribution (all chains having exactly the same length). This is an extremely idealized situation, and chemical irregularities such as polydispersity and branching are not unusual. Although branching is not commonly seen in the ionic addition polymerization process, the probability is larger for longer chains. Branching can sufficiently slow the molecular motion, as discussed

by de Gennes.[14]

The effect of polydispersity was discussed in Doi–Edwards' stress relaxation analysis.[3] Here, since the orientation relaxation is explained in terms of the fraction of initial tubes remaining, a similar analyses can be used. Let $P(M)$ be the molecular weight distribution and M_i and M_f be the limits of the distribution. Since in the present theory no interchain correlation is taken into account, each chain contributes to the orientation additively. Therefore, the average fraction of initial tubes remaining at time t can be expressed as

$$\langle F(t) \rangle = \int_{M_i}^{M_f} F_0(t) P(M)\, dM \qquad (14)$$

where $F_0(t)$ is the fraction of the chain remaining inside the initial tubes at time t for the idealized δ-function distribution of molecular weight as expressed in eq 8.

Since the molecular weight dependence of the normalized Hermans orientation function is strong, the effect of polydispersity would be significant even if the sample is nearly monodisperse.

To summarize this FT-IR study, we have concluded that (1) the stages of orientation relaxation can be characterized by using the evaporation of the tube from the initial non-Gaussian conformation to the final Gaussian conformation. This is achieved by the emergence and growth of the minor chain. (2) The scaling arguments seem to be supported by the experimental observations, but further work is needed to explain all the observations.

Acknowledgment. We are grateful to the National Science Foundation for the financial support of this work, Grant DMR 82-16181 (Polymers Program). Appreciation is also expressed to Brian Joss of the Materials Research Laboratory for his assistance in the preparation of the samples and to MRL for its support of the FTIR Facility, NSF-DMR-83-16981.

Registry No. Polystyrene, 9003-53-6.

References and Notes

(1) de Gennes, P. G. *J. Chem. Phys.* **1971**, *55*, 572.
(2) Edwards, S. F. *Proc. Phys. Soc., London* **1967**, *92*, 9.
(3) Doi, M.; Edwards, S. F. *J. Chem. Soc., Faraday Trans. 2* **1978**, *74*, 1789, 1802, 1818; **1978**, *75*, 32.
(4) de Gennes, P. G.; Leger, L. *Annu. Rev. Phys. Chem.* **1982**, *33*, 49.
(5) Kim, Y. H.; Wool, R. P. *Macromolecules* **1983**, *16*, 1115.
(6) Wool, R. P. *J. Elastomers Plast.* **1985**, *17*, 106.
(7) Graessley, W. W. *Adv. Polym. Sci.* **1982**, *47*, 67.
(8) Marrucci, G. *J. Polym. Sci., Polym. Phys. Ed.* **1985**, *23*, 159.
(9) Gaylord, R. J.; DiMarzio, E. A.; Lee, A.; Weiss, G. H. *Polym. Comm.* **1985**, *26*, 337.
(10) de Gennes, P. G. "Scaling Concepts of Polymer Physics"; Cornell University Press: Ithaca, NY, 1978.
(11) Fraser, P. D. B. *J. Chem. Phys.* **1953**, *21*, 1511.
(12) Hermans, J. J.; Hermans, P. H.; Vermaas, D.; Weidinger, A. *Recl. Trav. Chim. Pays-Bas* **1946**, *65*, 427.
(13) Jasse, B.; Koenig, J. L. *J. Polym. Sci., Polym. Phys. Ed.* **1979**, *17*, 799.
(14) de Gennes, P. G. *J. Phys.* **1975**, *36*, 1199.
(15) Boue, F.; Nierlich, M.; Jannink, G.; Ball, R. *J. Phys.* **1982**, *43*, 137.
(16) Narkis, M.; Hopkins, I. L.; Tobolsky, A. V. *Polym. Eng. Sci.* **1970**, *10*, 66.
(17) Cotton, J. P.; Decker, D.; Benoit, H.; Farnoux, B.; Higgins, J.; Jannink, G.; Ober, R.; Picot, C.; Des Cloizeaux, J. *Macromolecules* **1974**, *7*, 863.
(18) Plazek, J. D. *J. Phys. Chem.* **1965**, *69*, 95.

Surface Structure of Segmented Poly(ether urethanes) and Poly(ether urethane ureas) with Various Perfluoro Chain Extenders. An X-ray Photoelectron Spectroscopic Investigation

Sung Chul Yoon and Buddy D. Ratner*

National ESCA and Surface Analysis Center for Biomedical Problems, Center for Bioengineering and Department of Chemical Engineering, BF-10, University of Washington, Seattle, Washington 98195. *Received July 23, 1985*

ABSTRACT: Fluorine-containing segmented poly(ether urethanes) and poly(ether urethane ureas) based on 4,4′-methylenebis(phenylene isocyanate) (MDI) were synthesized by using 2,2,3,3-tetrafluoro-1,4-butanediol (FB), 2,2,3,3,4,4-hexafluoro-1,5-pentanediol (FP), 1,4-diaminotetrafluorobenzene (TFB), or 4,4′-diaminooctafluorobiphenyl (OFB) as chain extenders. The soft segment consisted of poly(tetramethylene glycol) (PTMO) of molecular weight 1000 or 2000. The characterization of polymers was carried out by bulk elemental analysis, gel permeation chromatography, infrared spectroscopy, and X-ray photoelectron spectroscopy (XPS). For the PTMO-2000-containing polymers, the angular dependence of the XPS signal demonstrated that the fluorine content decreases monotonically as one samples closer to the surface and approaches 80–100% of the bulk value at the maximum effective sampling depth (~100 Å). The FB chain-extended polymers have more soft segment at the surface than the FP chain-extended polymers at the same hard-segment content. A decrease in the soft-segment molecular weight from 2000 to 1000 produces an increase of fluorine content or hard-segment concentration in the surface region at the same level of hard-segment concentration. The FP chain-extended polymers based on PTMO-1000 show no angular dependence and have the same fluorine content uniformly distributed throughout the surface region and in the bulk. All of the XPS angular-dependent data indicate that the surface topography of segmented polyurethanes and poly(urethane ureas) strongly depends on the extent of phase separation.

Introduction

Although segmented polyurethanes represent an industrially important class of polymers and their bulk structure and mechanical properties have been extensively studied, the surface structure of these materials has been studied primarily in connection with their application in medical devices. In particular, it has been demonstrated that measurements of the surface composition of these polymers can be correlated with blood interactions.[1,2]

* To whom correspondence should be addressed

0024-9297/86/2219-1068$01.50/0